

Heterologous Expression of the Adenosine A1 Receptor in Transgenic Mouse Retina[†]

Ning Li,^{‡,⊥} David Salom,^{‡,⊥} Li Zhang,^{‡,#} Tim Harris,^{‡,△} Juan A. Ballesteros,^{‡,○} Marcin Golczak,[§] Beata Jastrzebska,[§] Krzysztof Palczewski,[§] Carole Kurahara,^{||} Todd Juan,^{||} Steven Jordan,^{||} and John A. Salon*^{||}

Novasite Pharmaceuticals Inc., San Diego, California 92121, Department of Pharmacology, Case Western Reserve University, Cleveland, Ohio 44106, and Amgen Inc., Thousand Oaks, California 91320

Received January 24, 2007; Revised Manuscript Received April 13, 2007

ABSTRACT: Traditional cell-based systems used to express integral membrane receptors have yet to produce protein samples of sufficient quality for structural study. Herein we report an in vivo method that harnesses the photoreceptor system of the retina to heterologously express G protein-coupled receptors in a biochemically homogeneous and pharmacologically functional conformation. As an example we show that the adenosine A1 receptor, when placed under the influence of the mouse opsin promoter and rhodopsin rod outer segment targeting sequence, localized to the photoreceptor cells of transgenic retina. The resulting receptor protein was uniformly glycosylated and pharmacologically well behaved. By comparison, we demonstrated in a control experiment that opsin, when expressed in the liver, had a complex pattern of glycosylation. Upon solubilization, the retinal adenosine A1 receptor retained binding characteristics similar to its starting material. This expression method may prove generally useful for generating high-quality G protein-coupled receptors for structural studies.

The vital role that G protein-coupled receptors (GPCRs)¹ play as gate keepers in cellular signaling and the broad spectrum of pathophysiologicals in which they are implicated make this protein superfamily a prominent focus of modern drug discovery (1–3). To date, the integral membrane nature of these proteins has precluded drug discovery campaigns based on their structures. Recently, however, the 3-D structures of the prototypical GPCR rhodopsin (4) and meta II-like rhodopsin (5) were reported [see progress in recent reviews (6, 7)]. These breakthroughs were facilitated in part by rhodopsin's highly enriched and homogeneous expression

in the photoreceptors of the retina from which the protein was purified (8).

Key elements of the photoreceptor expression system responsible for this success include a biosynthesis and transport pathway that has optimally evolved to deliver large amounts of rhodopsin to the retina's rod outer segment (ROS) organelle (4, 9, 10). The ROS organelle itself is a highly differentiated and specialized structure, consisting of an organized stack of folded and contiguous membrane layers that present a concentrated matrix of functional rhodopsin molecules to the light-sensing layer of the retina (4, 10). The ability of the photoreceptor system to support the biosynthesis and storage of such a highly concentrated depot of rhodopsin molecules has prompted us to explore its utility for the heterologous expression of GPCRs in general. Other efforts along these lines have been reported using *Drosophila* and *Xenopus* systems (11–13). Whereas genetic manipulation of both of these species is relatively simple, the resulting expression of gene products can be variable and unstable. Moreover, the small size of fly and tadpole eyes and the potentially eccentric characteristics of posttranslational processing in these nonmammalian organisms could undermine their usefulness for generating drug target proteins suitable for structural studies. For these reasons we were interested in developing a more stable and scalable mammalian system and elected to explore the design of an in vivo murine system for these purposes.

Here we report the engineering and characterization of transgenic mice that heterologously express fully functional adenosine subtype A1 receptor protein (AA1R) in their retinas. We describe the localization of these receptors in the retina's substrata, their biochemical homogeneity, and

[†] This research was supported in part by U.S. Small Business Innovation Research (SBIR) Grant R44MH068919 from the National Institute of Mental Health (NIMH) and Grant R44DA016476 from the National Institute of Drug Abuse (NIDA), National Institutes of Health, Bethesda, MD.

* Address correspondence to this author. Phone: 805-447-6442. Fax: 805-447-1331. E-mail: jsalon@amgen.com.

[‡] Novasite Pharmaceuticals Inc.

[§] Case Western Reserve University.

^{||} Amgen Inc.

[⊥] Current address: Polgenix Inc., 11000 Cedar Ave., Cleveland, OH 44106.

[#] Current address: Forbes Medi-Tech Inc., 10931 North Torrey Pines Road, La Jolla, CA 92037.

[△] Current address: SAIC-Frederick Inc., NCI, P.O. Box B, Frederick, MD 21702.

[○] Current address: OrphaMed S.L., Parque Científico de Madrid, 28760 Tres Cantos, Madrid, Spain.

¹ Abbreviations: AA1R, adenosine subtype A1 receptor; (m)Ab, (monoclonal) antibody; CP-55,940, (–)-*cis*-3-[2-hydroxy-4-(1,1-dimethylheptyl)phenyl]-*trans*-4-(3-hydroxypropyl)cyclohexanol; CPX, 8-cyclopentyl-1,3-dipropylxanthine; DM, *n*-dodecyl β-D-maltoside; DPCPX, 1,3-dipropyl-8-cyclopentylxanthine; GPCR, G protein-coupled receptor; NECA, 5'-*N*-ethylcarboxamidoadenosine; RHO₁₅, 15 amino acid long C-terminal region of opsin; ROS, rod outer segment; XAC, xanthine amine congener, 8-[4-[[[(2-aminoethyl)amino]carbonyl]methyl]oxy]phenyl]-1,3-dipropylxanthine.

pharmacological activity as evidence for their successful functional expression.

EXPERIMENTAL PROCEDURES

Preparation of the AA1R Construct. The transgenic mouse expression plasmid for AA1R was constructed as follows: a pXOP-C1(-) vector originally constructed to target retinal expression in *Xenopus laevis* (13) was cut by *NotI/XhoI* to remove the *Xenopus* opsin promoter sequence and replaced with a 5 kb mouse opsin promoter (14–16). DNA fragments encoding an 11 amino acid long tag (MASMTGGQMG) corresponding to the N-terminal region of the major capsid protein from the T7 bacteriophage (T7) and a 15 amino acid long tag (SATASKTETSQVAPA) containing the ROS targeting sequence found in the C-terminal region of mouse opsin (RHO₁₅) were then inserted to produce the parental mouse expression vector pNova-T1 (17, 18). The full-length coding sequence for AA1R was generated by RT-PCR using *pfu* polymerase (Stratagene, La Jolla, CA). Amplimers designed from the Genebank accession file of human AA1R (X68485) included a perfect Kozak site prior to the start codon. The blunt-ended amplified product was inserted into the *PmeI* site of pNova-T1 to generate the recombinant vector pNova-T1-AA1R-T7-RHO₁₅, which was then used to generate transgenic mouse lines.

Generation of Transgenic Mice. The recombinant expression construct was linearized and gel-purified prior to microinjection into 18-h-old FVB/NTac or C57BL/6NTac embryos (Taconic, Germantown, NY) which were then implanted into pseudopregnant females to produce founder stock (19). These animals were screened for the presence of the transgene by assaying genomic DNA prepared from tail tissue by use of a NucleoSpin tissue HC binding plate (Macherey-Nagel, Duren, Germany) on a Muti-Probe II Plus robot (Perkin-Elmer, Wellesey, MA). Initial genotyping was conducted by PCR with primers selective for SV40 sequences (2150-54, 5'-GATGAGTTTGGACAAACCACA-3', and 2150-55, 5'-CCGGATCATAATCAGCCATAC-3'), which should selectively incorporate only into transgene positive animals (20). The presence of specific exogenous receptor genes was subsequently confirmed by employing primers directed to AA1R (AA1R-f: 5'-GCCACCATGCCGCCCTC-3') and Rho₁₅tag (Mops-A1: 5'-TTAGGCTGGAGCCACCTGGC-3'). Genotype positive male founders were then bred with 6-week-old wild-type C57BL/6 females (Jackson Laboratory, Bar Harbor, ME) to produce F1 lines.

Generation of Cell Culture Controls. HEK293T cells (ATCC, Manassas, VA) were grown under 5% CO₂ in Dulbecco's modified Eagle's medium containing 5% fetal calf serum and 0.38 g/L L-glutamine. Sequences encoding the 11 amino acid long T7 and 15 amino acid long RHO₁₅ tags were inserted into the multicloning site of pcDNA4TO (Invitrogen, Carlsbad, CA) to create the vector pcDNA4TO/T7-RHO₁₅. In an arrangement analogous to the mouse transgenic expression vector, the full-length AA1R cDNA was then subcloned into this vector upstream of the T7-RHO₁₅ tag, and the sequence was verified. The resulting pcDNA4/AA1R-T7-RHO₁₅ vector was used to transiently transfect HEK293T cells using Lipofectamine 2000 reagent (Invitrogen). Cells were collected 48 h after transfection for subsequent study.

Immunoblotting and Quantification. Mouse retinas were homogenized by polytron (30 s on ice) in 10 mM HEPES, pH 7.4, containing protease inhibitor cocktail (Sigma Aldrich, St. Louis, MO). The crude retinal membrane pellet was recovered by centrifugation (25000g for 30 min, 4 °C) and solubilized in 40 mM *n*-dodecyl β -D-maltoside (DM). Insoluble material was removed by centrifugation (25000g for 30 min) and the cleared supernatant recovered. HEK293T cells were collected by scraping 48 h posttransfection. After being washed once with phosphate-buffered saline, pH 7.4 (PBS), they were homogenized as above, and a crude membrane pellet was collected by centrifugation (40000g for 30 min, 4 °C) (21). Samples were subjected to SDS-PAGE and transferred to nitrocellulose by electroblotting. The nitrocellulose transfer was blocked with 5% nonfat dry milk in 0.05% Tween 20 and Tris-buffered saline, pH 7.4 (TBST), and incubated with mouse anti-T7 antibody (EMD Bioscience, San Diego, CA) diluted 1:2000 in TBST at 4 °C overnight. After washing, nitrocellulose membranes were incubated for 1 h with HRP-conjugated anti-mouse IgG (Pierce Biotechnology, Rockford, IL), diluted 1:5000, and then washed and incubated with SuperSignal extended duration chemiluminescent substrate (Pierce Biotechnology, Rockford, IL) for 5 min. Signals were detected with a UVP CCD camera and quantified by densitometric scan (Lab-Works image acquisition and analysis software). Total amounts of heterologous AA1R protein present in transgenic retinas were estimated by a semiquantitative immunoblotting protocol which employed a standard curve of AA1R protein purified from HEK293T cells stably transfected with the AA1R-T7-RHO₁₅ construct. AA1R was purified from cells by immunoaffinity chromatography with an anti-1D4 mAb directed to the 9 amino acid long region of opsin contained within the RHO₁₅ tag (18). Postchromatography material was deglycosylated by incubation with 5 units of *N*-glycosidase F (PNGase F; Calbiochem, San Diego, CA) for 1 h at room temperature. The amount of receptor protein present was estimated after SDS-PAGE and silver staining by densitometric comparison to a bovine serum albumin reference curve.

Histology. Retinas were dissected immediately from sacrificed mice, fixed in freshly prepared 4% paraformaldehyde in PBS for 2–3 h at 4 °C, washed in 5%, 10%, 15%, and 20% SPB (sucrose phosphate buffer, pH 7.5), equilibrated in 20% SPB/OCT (OCT compound; Miles Laboratories, Elkhart, IN) (2:1) at 4 °C overnight, and finally embedded in 20% SPB/OCT (2:1) on dry ice. Embedded retinas were cryosectioned and counterstained with hematoxylin and eosin (HE) to reveal retinal structures by light microscopy (22).

Immunocytochemistry. Cryosections of mouse retina were postfixated in cold acetone-methanol (1:1), rinsed in PBS, and blocked with 10% goat serum/PBS. Either B6-30N mAb diluted at 1:400 (23) or T7 mAb diluted at 1:200 was used as the primary antibody. Cy3-conjugated goat anti-mouse IgG diluted at 1:200 was used as the secondary antibody. Nuclei were counterstained with 1 μ g/mL Hoechst 33342. Signals were visualized by fluorescence microscopy at excitation/emission wavelengths (nm) of 550/570 for Cy3 and 350/461 for Hoechst 33342. For hepatic immunocytochemistry, liver tissue was fixed in 4% paraformaldehyde for 18 h, incubated in increasing concentrations of sucrose

(5–20%) in PBS, and then embedded in 50% SPB/OCT diluted with 20% sucrose in PBS. Sections were cut at 10 μm and incubated with 1.5% normal goat serum in PBST (PBS with 0.1% Triton X-100) for 15 min at room temperature. The sections were then incubated overnight at 4 $^{\circ}\text{C}$ with purified mouse anti-1D4 mAb, rinsed in PBST, and incubated with Cy3-conjugated goat anti-mouse IgG or goat anti-rabbit IgG for detection of opsin immunofluorescence. Sections were visualized with a Leica DM6000 B microscope.

Pharmacology. Samples were prepared for pharmacology studies as follows: Cultured cells were washed once with PBS, harvested by scraping into lysis buffer (25 mM HEPES, pH 7.4, 1 mM EDTA, protease inhibitor cocktail), homogenized with a polytron (30 s on ice), and centrifuged (25000g for 30 min, 4 $^{\circ}\text{C}$). Resulting crude membrane pellets were resuspended in binding buffer (25 mM HEPES, pH 7.4, 1 mM EGTA, 2 mM MgCl_2). Retinas from 28–30-day-old mice were harvested by dissection, suspended directly in binding buffer, and homogenized by polytron (30 s on ice), and the total homogenates were used to minimize loss of receptors. Radioligand binding assays of either crude cell membranes or total retinal homogenates were performed in 96-well plates in a final volume of 200 μL per well. Binding mixtures were incubated at room temperature with shaking for 60 min, and free radioligand was removed by filtration over Whatman GF/C filter plates using a Brandel cell harvester. After addition of scintillation cocktail, receptor-bound radioactivity was measured using a TopCount scintillation counter. Saturation binding curves were generated for AA1R using [^3H]DPCPX, with nonspecific binding measured in the presence of 10 μM N^6 -cyclopentyladenosine. For competitive displacement studies, varying concentrations of test ligands were preincubated with receptor material in binding buffer for 30 min prior to addition of radioligand, which was then allowed to incubate for an additional 60 min. B_{max} and K_d values were calculated by a nonlinear regression curve fit via the GraphPad Prism program. IC_{50} values were determined by a nonlinear regression curve fit and transformed to K_i using the Chang–Prusoff correction. All experiments were performed in triplicate.

Immobilization of AA1R-T7-RHO₁₅ Fusion Protein to Affinity Resin. Total receptor protein was prepared by homogenizing 40 whole eyes harvested from AA1R-T7-RHO₁₅ expressing mice in binding buffer containing protease inhibitors and 10 units/mL DNase (Sigma Aldrich). Membranes were recovered by centrifugation (100000g, 30 min, 4 $^{\circ}\text{C}$), washed with binding buffer, and solubilized in 0.8 mL binding buffer containing 10 mM DM, protease inhibitor cocktail, and 10 units/mL DNase with rocking at 4 $^{\circ}\text{C}$ for 30 min. Insoluble material was removed by centrifugation (100000g, 30 min, 4 $^{\circ}\text{C}$). The resulting supernatants containing detergent-solubilized AA1R-T7-RHO₁₅ fusion protein were captured by rocking incubation with 100 μL of 1D4 mAb–Sepharose gel suspension for 60 min at 4 $^{\circ}\text{C}$. Batch incubations were washed six times with 1 mL of wash buffer (1 mM CHAPS, 25 mM HEPES, pH 7.4). Radioligand binding assays with AA1R-T7-RHO₁₅ bound to Sepharose gel were performed as described above. A similar procedure was used to prepare and test AA1R-T7-RHO₁₅ expressed in HEK293T cells as controls.

Generation of Opsin Liver Expressing Transgenic Mice. A hepatocyte transthyretin (TTR) minigene construct (a gift from Dr. Robert H. Costa from the University of Illinois) was used to ensure proper targeting and exclusive expression of opsin in the liver (24). Mouse opsin cDNA was amplified with primers 5'-GCAGATAGGCCTATGAACGGCACA-GAGGGCC-3' and 5'-GCAGATAGGCCTTTAGGCTG-GAGCCACCTGG-3', blunt ended, and ligated into a unique *StuI* site located in the second exon of the TTR minigene vector. The construct was sequenced, and a 5.5 kb *HindIII* fragment containing the 3 kb TTR promoter driving opsin cDNA expression was separated from the vector by agarose electrophoresis, purified, and used to generate transgenic mice as described above. Identification of mice carrying the transgene was performed as described above using primers complementary to the opsin cDNA sequence (5'-ATGAACGGCACAGAGGGCC-3' and 5'-TTAGGCTGGAGCCACTGG-3').

Purification of Isorhodopsin. Transgenic mice were gavage twice (16 and 3 h before sacrifice) with 2 mg of 9-*cis*-retinal suspended in 100 μL of sunflower seed oil and dispatched, and their livers were homogenized in PBS containing 20 mM DM. The solubilized homogenate was cleared by centrifugation (125000g at 4 $^{\circ}\text{C}$ for 1 h) and used to purify isorhodopsin by 1D4 immunoaffinity chromatography as described previously (25, 26).

Deglycosylation and Immunoblotting of Opsin. Approximately 0.5 μg of purified isorhodopsin purified from liver was incubated with 500 units of peptide-*N*-glycosidase F or Endo H for 3 h at room temperature according to the supplier (New England BioLabs).

Gt Activation. Assays were performed on purified rhodopsin as described elsewhere (26).

RESULTS

Genetic Engineering of Transgenic Mice. The AA1R transgene construct consisted of five fragments: (1) a previously characterized mouse opsin promoter containing a 5 kb sequence upstream of the start codon, (2) a full-length AA1R coding sequence, (3) a sequence coding for the initial 11 amino acids of the T7 gene 10 protein which is the epitope for the T7 antibody, followed by (4) a sequence encoding the 15 residue long C-terminal region from mouse opsin containing the ROS-targeting signal and epitope for the anti-1D4 mAb and, finally, (5) an SV40 derived polyadenylation site (27) (Figure 1A).

Two strains of mice, FVB/N and C57BL/6, were employed to generate the transgenic lines. Upon genotyping, a total of 28 transgene positive male founders were recovered for AA1R. These positive male founders were then bred with C57BL/6J wild-type females to generate F1 animals for further analyses.

Protein Expression. Retinas harvested from transgene positive F1 animals and wild-type littermates were tested for the presence of the AA1R-T7-RHO₁₅ fusion protein by immunoblot analysis with anti-T7 mAb. Animals were ranked on the basis of the intensity of the anti-T7 signal, which was taken as an indicator of total receptor protein content. By this criterion, F1 offspring from the AA1R transgenic founder F73 showed the highest expression level of total receptor protein. A representative blot of this sample

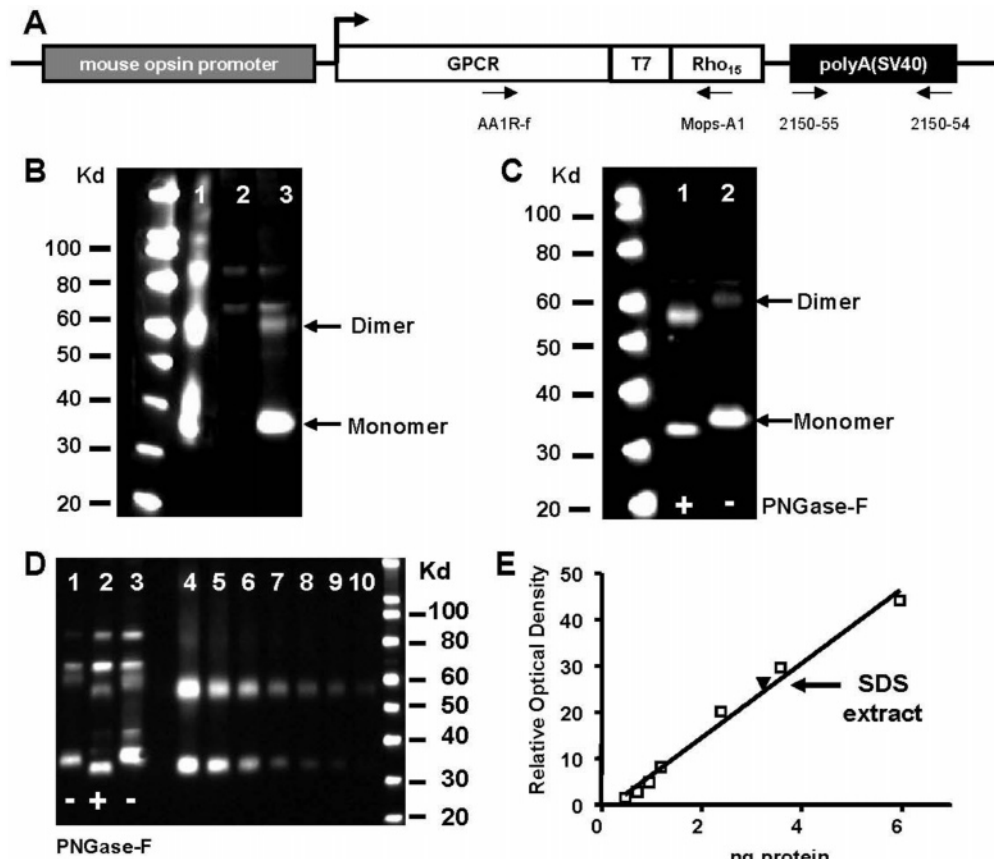


FIGURE 1: Immunoblotting of AA1R-T7-RHO₁₅ transgenic mouse retina (F1 offspring from founder F73) and total AA1R-T7-RHO₁₅ protein estimated by immunoblotting. (A) AA1R-T7-RHO₁₅ transgene construct. Retinal expression of the heterologous AA1R fused to T7 and RHO₁₅ tags flanked by an SV40 polyadenylation site is driven by a 5 kb mouse opsin promoter sequence positioned upstream of the GPCR start codon. Approximate locations of genotyping primers are indicated by arrows. (B) DM (*n*-dodecyl β -D-maltoside) extracts of total membrane protein from HEK293T cells transiently transfected with AA1R (lane 1) and retinas from transgenic mice (lane 3, >95% monomeric protein) and their wild-type littermates (lane 2). The blot was probed with T7 antibody. (C) DM extracts of transgenic retina before (lane 2) and after (lane 1) incubation with PNGase F and probed with T7 antibody. The equivalent of \sim 7% of a mouse retina was loaded onto each lane. (D) DM (lanes 1 and 2) or SDS (lane 3) extracts of retinas from transgenic mice were loaded with different amounts (lanes 4–10) of deglycosylated AA1R-T7-RHO₁₅ protein purified from a stable HEK293T cell line. The blot was probed with T7 antibody. The equivalent of \sim 3.5% of a mouse retina was loaded in lanes 1–3. Protein profiles of DM extracts of transgenic retina are shown before (lane 1) and after (lane 2) incubation with PNGase F. (E) A standard curve generated from lanes 4–10 was analyzed with UVP BioImaging Systems and Prism software and used to estimate the amount of protein present in retinal extracts.

(Figure 1B) indicates that T7 immunoreactivity was present only in samples prepared from transgenic retina, and the electrophoretic mobility corresponded to a predicted molecular weight of the fusion protein. The electrophoretic mobility of the retinal-expressed protein also appears to be less diffuse than that of an analogous construct conventionally expressed in HEK293T cells, suggesting that a more consistent degree of glycosylation is afforded by the retinal rod cells. This is further supported by treatment with glycosidase, which increased the mobility without affecting the sharpness of the band (Figure 1C). The total amount of transgene receptor protein present in the retina was estimated by a semiquantitative immunoblotting protocol. By this method it was determined that approximately 90 ng of total AA1R protein was present in each retina of F73 offspring (see Figure 1D,E).

To test whether or not glycosylation of opsin is uniform in mouse organs other than rod cells, we examined its biochemical characteristics when heterologously expressed in the liver. Upon examination, it was found that opsin successfully reached the plasma membrane with apparently little or no protein held up in the Golgi or ER (Figure 2A).

Opsin can be regenerated *in vivo* by oral administration of 9-*cis*-retinal to form isorhodopsin. Immunoaffinity purification yielded approximately 100 μ g of isorhodopsin from 1 g of liver. The UV-vis spectrum of the purified isorhodopsin (with A_{\max} at 494 nm) revealed a characteristic blue shift as compared to rhodopsin (28) (Figure 2C). The higher ratio of 280 nm (protein absorbance peak) to 500 nm (chromophore) suggests the presence of a copurifying nonprotein liver-specific contaminant that bound either to the resin or to opsin itself, because the silver-stained SDS-PAGE gel showed no other contaminating proteins (Figure 2C, insert). This material was not present in mouse eyes as the ratio was <1.8 (data not shown). The purified protein can be completely bleached with light, leading to chromophore release as indicated by a shift of A_{\max} to 360 nm. Purified isorhodopsin activated Gt α in the direct intrinsic fluorescence assay with an initial activation rate [$k_0 = 1.5 \text{ e}^{-3} (\text{s}^{-1})$] comparable to rates calculated under similar conditions for native bovine rhodopsin (29) (Figure 2D). These results indicate that opsin expressed in the liver is correctly folded and fully functional. By SDS-PAGE analysis, what appears to be a monomeric form of opsin

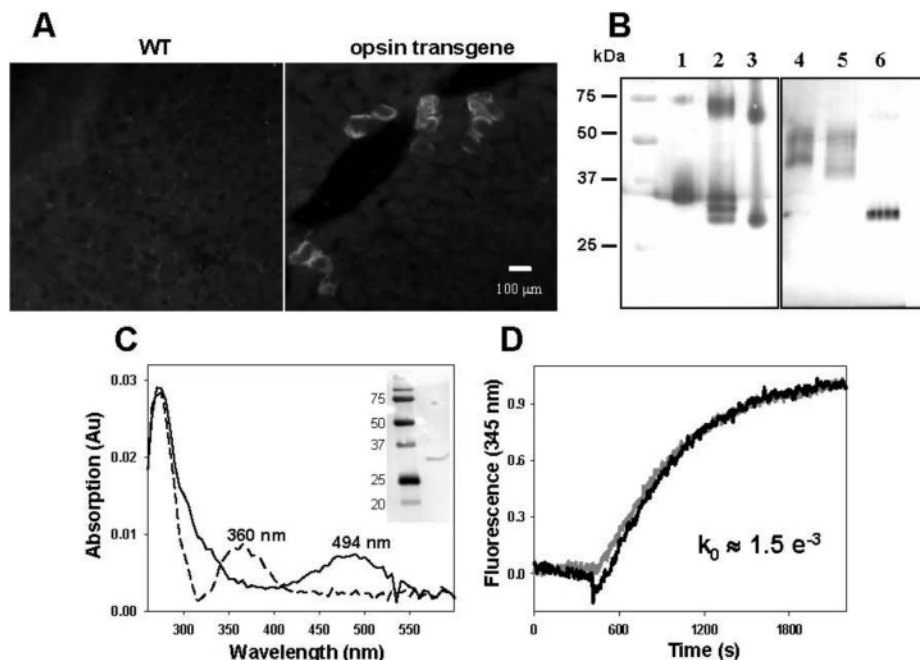


FIGURE 2: Properties of opsin heterologously expressed in mouse liver. (A) Immunocytochemistry of transgenic mouse liver showing positive expression of opsin in the left panel. (B) Immunoblotting of SDS-PAGE resolved purified opsin before (lane 4) and after treatment with Endo H (lane 5) or peptide:*N*-glycosidase F (lane 6). Lane 1, 2, and 3 controls show native bovine rhodopsin before and after treatment with Endo H or PNGase F, respectively. (C) UV-vis absorbance spectra of isorhodopsin purified from mouse liver before (solid line) and after (dotted line) bleaching in the presence of 20 mM NH_2OH . Absorbance maxima at 494 and 360 nm are characteristic for opsin regenerated with 9-*cis*-retinal and retinoid released from the opsin binding site, respectively. The insert shows silver staining of isorhodopsin used for spectral analysis. (D) Gt activation by purified isorhodopsin was monitored by the increase in fluorescence of the Gt_α subunit at 345 nm. The initial rate calculated as a pseudo-first-order reaction [$k_0 \approx 1.5 \text{ e}^{-3} (\text{s}^{-1})$] is comparable to the value obtained for bovine native rhodopsin (gray line) (29).

migrated as a broad band (40–75 kDa) caused by heterogeneous *N*-linked glycosylation as demonstrated by treatment with Endo H or peptide:*N*-glycosidase F (Figure 2B). By comparison to the ROS-derived receptor protein, these data suggest that the photoreceptors may be unique in their ability to produce GPCRs with a highly homogeneous pattern of glycosylation.

Retinal Morphology and Receptor Localization. Transgenic mouse lines with detectable levels of AA1R-T7-RHO₁₅ fusion protein, as shown by immunoblotting, were examined for retinal morphology by hematoxylin and eosin staining (HE). The highest expression of the fusion protein was observed in 25–30-day-old mice by immunoblotting (data not shown). We therefore elected to harvest retinas from F1 mice at 28 days, which in wild-type animals is a point at which retinas are fully developed (7). Upon examination, retinal sections of AA1R's F73-derived F1 offspring showed that the ROS layer was absent and that there were fewer layers of nuclei in the outer nuclear layer (ONL) as compared to wild-type retina (Figure 3, panel D vs panel A). Although the ROS was absent, the AA1R-T7-RHO₁₅ fusion protein could still be detected in both the outer nuclear layer (ONL) and inner segment (IS) by immunocytochemistry (Figure 3, panel F vs panel C).

Pharmacology. Demonstration of predictable receptor-specific pharmacology can be taken as evidence that the heterologous receptor protein has been correctly processed and inserted into retinal membranes in a functional conformation. Accordingly, AA1R radioligand binding assays were conducted on retinal and cell culture derived samples. Saturation binding curves generated with the AA1R-specific antagonist [³H]DPCPX were similar for total homogenates

prepared from AA1R transgenic retina and crude membranes prepared from AA1R-transfected HEK293T cells (Figure 4) (30, 31). In both instances the levels of specific binding appeared to be comparable as did the K_d values (AA1R retina, K_d 6.9 nM; AA1R HEK293T, K_d 1.9 nM).

Scatchard analysis of these binding isotherms indicated that AA1R binding sites were present at a B_{max} of 2.1 pmol/mg of protein in total homogenates prepared from transgenic retina as compared to 3.2 pmol/mg of protein in membrane fractions prepared from transfected HEK293T cells. Considering the total amount of receptor protein present, as estimated by immunoblotting, the B_{max} observed for retina suggests that approximately half of the receptor protein is available for ligand binding (the equivalent of ~ 37 ng based on 2.1 pmol of AA1R binding sites/mg of retina protein, a molecular mass for AA1R of 40 kDa, and a yield of ~ 0.4 mg of total protein per retina). These estimates are impacted by differences in sample processing and possible masking of binding sites due to formation of inside-out membrane vesicles. By comparison, the levels of heterologous receptor observed in the engineered photoreceptor expression system are roughly equivalent to what could be achieved through conventional mammalian cell expression systems. In our experiments, the amount of AA1R protein present in one transgenic F73 retina is roughly equal to the amount of receptor protein generated by 25×10^6 transfected HEK293T cells expressing AA1R at a B_{max} of 3.2 pmol/mg of total membrane protein (based on ~ 0.5 mg of total membrane protein yield per 25×10^6 cells).

Displacement profiles were constructed using compounds considered to be diagnostic of AA1R pharmacology. The rank order of potency (CPX > XAC > NECA) and absolute

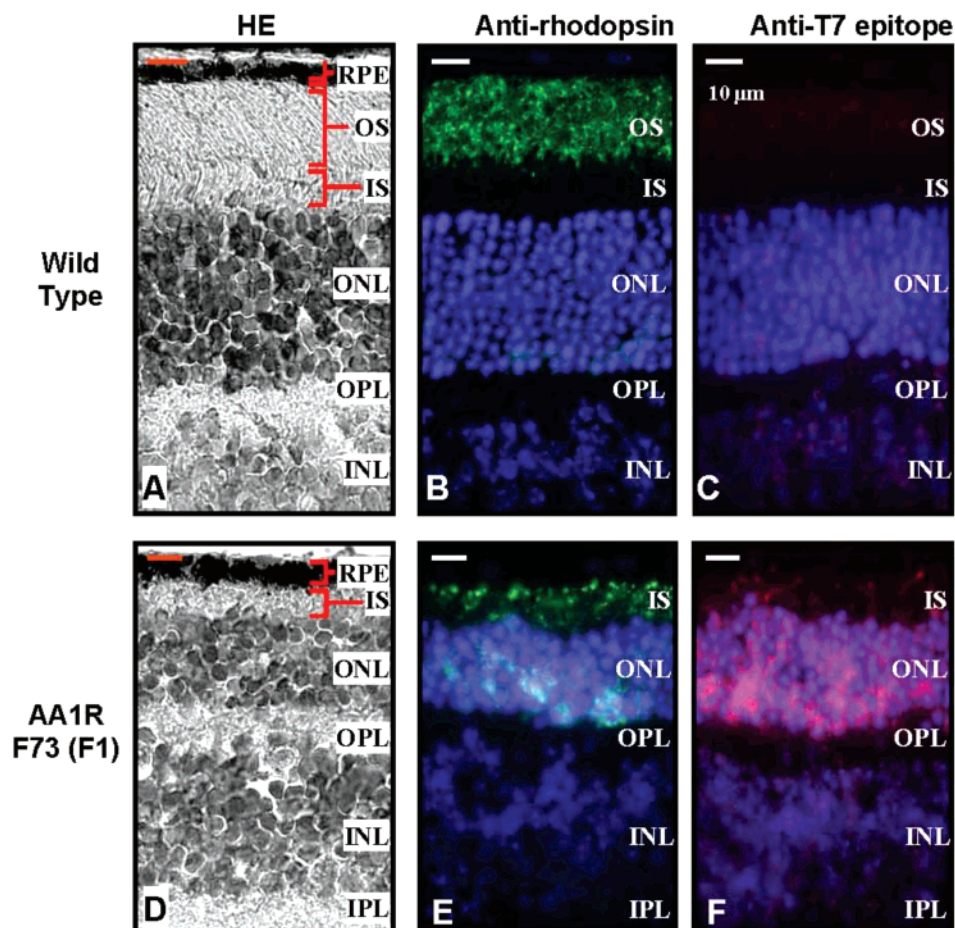


FIGURE 3: Retinal morphology and immunostaining of a typical retina section from F1 AA1R transgenic mice derived from transgenic founder F73. Hematoxylin and eosin staining revealed the retinal morphology of AA1R transgenic mouse (D) and its wild-type littermate (A). Immunostaining showed the expression of rhodopsin (in green, B, E) and AA1R-T7-RHO₁₅ (in red, C, F) in the retina of AA1R transgenic mice (E, F) and wild-type controls (B, C). Abbreviations: RPE, retinal pigmented epithelium; OS, outer segments; IS, inner segments; ONL, outer nuclear layer; OPL, outer plexiform layer; INL, inner nuclear layer; IPL, inner plexiform layer.

affinities (NECA, K_i 24 μ M; XAC, K_i 24–35 nM; CPX, K_i 3.5–6.1 nM) for both retinal and HEK293T samples were comparable to each other and similar to values reported in the literature (30, 32).

We also tested whether AA1R retained its basic binding characteristics after immobilization to a solid support of the type that might be used for its purification. In addition to ensuring that we could retain or regenerate a pharmacologically relevant receptor conformation, this experiment was important in demonstrating the ability to displace any copurifying endogenous or exogenously introduced stabilizing ligand prior to cocrystallization experiments. Because the linkage of the solubilized GPCR to the immunoaffinity resin occurs via the receptors' cytoplasmic C-terminal region, we expected that all receptor bound to the resin would present an unobstructed antagonist binding site. Examination of the binding isotherm for the immobilized receptor supports this conclusion and shows that saturation with [³H]DPCPX was virtually identical for solubilized AA1R purified from HEK293T cells and retinal rod cells (Figure 5) and had similar affinity for the radioligand as seen with the membrane-bound receptor (Figure 4).

The comparable levels of specific saturable ligand binding, radioligand K_d s, and similar profiles of rank order reference compound potencies observed for either membranous or immobilized receptor prepared from transgenic retina and

HEK293T material together suggest that the conformation of the AA1R is pharmacologically similar in both systems and confirm that proper folding and membrane insertion is occurring in the mouse photoreceptor expression system.

DISCUSSION

Although few in number, the majority of membrane protein structures deposited in the PDB are derived from crystals of abundant endogenous proteins purified from their natural sources. Most membrane proteins of pharmacological interest, however, exist at low levels in their native tissues, undermining the usefulness of native tissues as sources of starting material for purification campaigns. Conversely, it is unclear why crystallization of membrane proteins that have been heterologously expressed at high levels and purified from conventional *in vitro* cell-based systems has proven to be so difficult. To reconcile this apparent paradox, we postulated that there may be some subtle characteristics of isolated proteins that are crucial to formation of diffracting crystals. For example, a significant fraction of protein produced in traditional bacterial, yeast, insect, or mammalian cell systems is heterologously glycosylated or not glycosylated at all. As such, it is often diverted to inclusion bodies or the Golgi apparatus where it remains as misfolded aggregates. Both phenomena can undermine attempts to crystallize the purified protein.

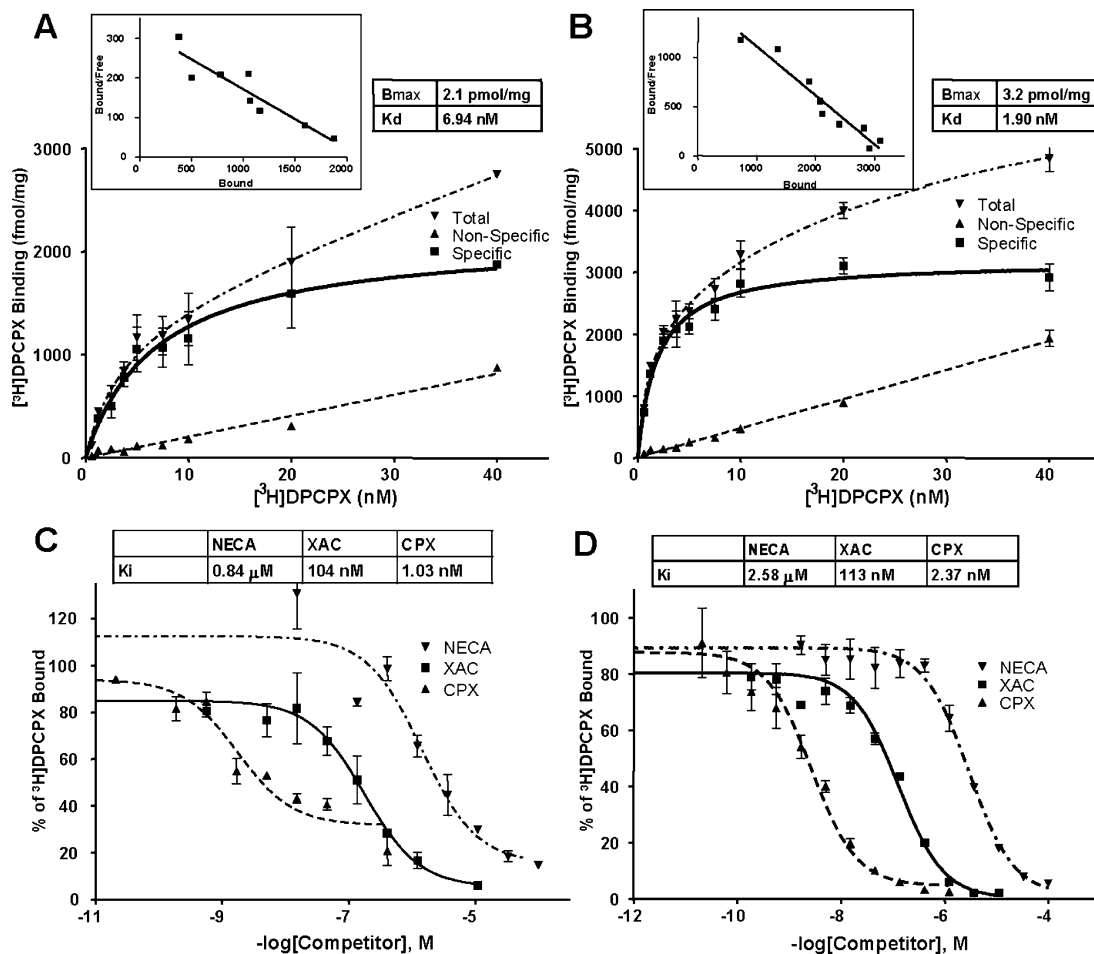


FIGURE 4: Ligand binding study of AA1R fusion proteins from mouse retina and HEK293T cells. (A, B) Saturation binding of the AA1R selective antagonist [3H]DPCPX to AA1R-T7-RHO₁₅ from (A) crude retinal homogenate or (B) HEK293T cell membranes. Data represent an average of two (A) or three (B) separate experiments with $n = 3$ replicates for each point. Error bars show standard deviations. Top left inserts: B_{max} and K_d values were derived from Scatchard analysis of the saturation curves as shown. Competition of adenosinergic compounds for [3H]DPCPX binding to AA1R-T7-RHO₁₅ from mouse retina (C) or HEK293T cells (D). Data show results from two (C) or three (D) independent experiments. Abbreviations: CPX, 8-cyclopentyl-1,3-dipropylxanthine; DPCPX, 1,3-dipropyl-8-cyclopentylxanthine; NECA, 5'-*N*-ethylcarboxamidoadenosine; XAC, xanthine amine congener, 8-[4-[[[(2-aminoethyl)amino]carbonyl]methyl]oxy]phenyl]-1,3-dipropylxanthine.

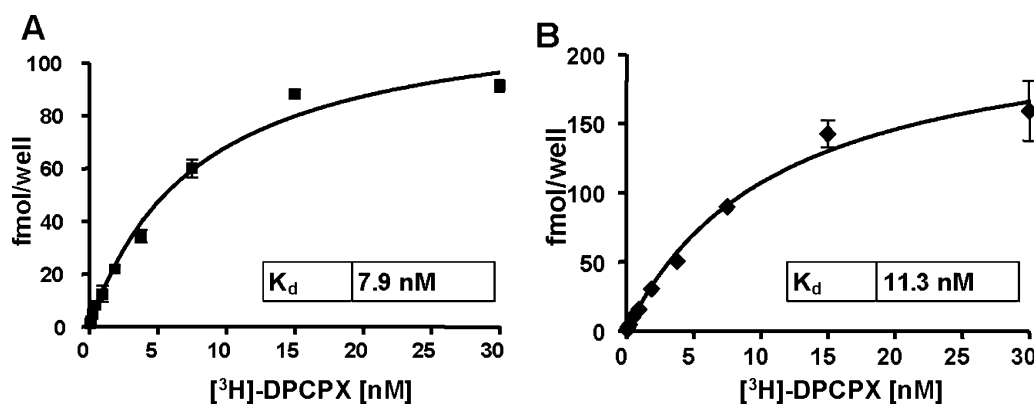


FIGURE 5: Ligand binding study of detergent-solubilized AA1R fusion protein purified from either transgenic mouse retina or HEK293T cells using 1D4 antibody-conjugated Sepharose gel. (A) Saturation binding of the AA1R selective antagonist [3H]DPCPX to AA1R-T7-RHO₁₅ from mouse retina bound to 1D4 antibody-conjugated Sepharose gel. (B) Saturation binding of the AA1R selective antagonist [3H]DPCPX to AA1R-T7-RHO₁₅ from HEK293T cells bound to 1D4 antibody-conjugated Sepharose gel. Data show the results from three independent experiments. Abbreviations: DPCPX, 1,3-dipropyl-8-cyclopentylxanthine.

The persistence of this problem is certainly not for want of efforts made to solve it. For example, one study which addressed the issue of heterogeneity of GPCR glycosylation (33, 34) found that a mutant HEK293 cell lacking *N*-

acetylglucosaminyltransferase I (GnTI) activity while capable of producing uniformly glycosylated rhodopsin did not generate protein crystals that could diffract to a similar resolution as the material obtained from the native retina.

On a different front, attempts made by the MepNet consortium to apply an industrial scale commitment to the GPCR crystallography problem documented the successful expression of more than 100 GPCRs using conventional expression systems such as *Escherichia coli*, *Pichia pastoris*, and Semliki Forest virus (SFV) vectors but did not report any successful crystallization trials (35).

Accordingly and in an effort to mimic nature's highly efficient expression of opsin, the only successfully crystallized GPCR prototype, we attempted to harness its *in vivo* expression apparatus to produce heterologous GPCR targets at will. Herein we have documented the first steps toward this goal by engineering transgenic mouse lines that express heterologous GPCRs in their retina. At the outset of this work, we considered both knock-in and transgenic approaches to produce genetically engineered mice that heterologously express high-quality GPCR protein in the retina's rod outer segment (ROS) apparatus. Whereas a knock-in approach should theoretically replace all endogenous rhodopsin protein with the heterologous GPCR protein and result in a homogeneous population of heterologous GPCR protein in the ROS, we anticipated that the requisite breeding steps would take a relatively long time to complete. Moreover, an attempt by another laboratory to express the endothelin receptor by such a knock-in approach was not successful (36). Conversely, we felt that a transgenic approach, which should result in the coexpression of heterologous GPCR target along with endogenous rhodopsin, should more quickly yield proof-of-concept results. Isolation of the GPCR target proper from the background rhodopsin could subsequently be addressed during ensuing purification trials. Accordingly, we report our initial observations with the quicker transgenic route.

In this paper we show that the receptor protein produced in our transgenic mice is present in a pharmacologically relevant conformation and appears homogeneously glycosylated. Whereas the presence of pharmacological activity is obviously relevant to biophysical examinations of receptor function, the importance of glycosylation for enabling such studies is less well defined. We can, however, infer something of glycosylation's importance from observations of the rhodopsin system. For example, it is known that the nature and extent of such posttranslational modifications are critical to the proper folding and function of rhodopsin and that modification of either of its two N-linked glycosylation sites results in defective transport to the cell surface. Such transport defects in turn adversely affect the stability of the ROS structure and result in impaired retinal function (37, 38). Interestingly, some evidence suggests that a tenuous but highly specific interaction of such carbohydrate moieties is critical for lattice formation during crystallization (5, 39). Thus it seems reasonable that an engineered GPCR expression system that provides a tightly controlled glycosylation pattern could be a useful tool in preparing samples for biophysical study, especially crystallography.

The usefulness of the photoreceptor expression system also depends on the amount of starting tissue that can be harvested and the relative level of target protein present therein. In this regard, the availability of stable and easily scaled-up breeding populations would seem advantageous. But, the causes and practical ramifications of the diminished levels of ROS we observed during these first engineering attempts

must also be considered. For example, it is unclear what, if any, relationship exists between the developmental integrity of the retina and the overexpression of a heterologous GPCR. Similarly, it is unknown what competitive pressure such heterologous expression may place on the retina's expression of native rhodopsin which in itself may be important for retinal development (40). Experimental observations suggest that altering the natural level of opsin expression can have a negative impact on the integrity of the retina. For example, heterozygous animals that are rhodopsin^{+/-} develop smaller ROS than wild-type animals (41), whereas homozygous rhodopsin^{-/-} knockout mice fail to form ROS altogether (40). Interestingly, retinal degeneration has been shown to accompany overexpression of human rhodopsin in mouse retina (42). Such observations suggest that whereas a naturally robust expression of rhodopsin is required for retinal integrity, attempts to exceed this level may inhibit vectorial transport of rhodopsin from the inner segment to the ROS and subsequently affect the viability of both the ROS and the retina at large. From a developmental standpoint it is unclear if the lack of ROS structures in our engineered strains is a manifestation of (a) retarded maturation or (b) accelerated degeneration of the retina. This suggests the possibility that improved retinal samples might be obtained by harvesting eye tissues outside the 25–30-day postnatal time point considered optimum for wild-type animals. Moreover, the effect of the T7 epitope on retinal integrity should also be explored.

While the quality of receptor protein appears good, the absolute amount of receptor protein present in the engineered retina was less than what our designs to mimic *in vivo* rhodopsin levels had promised. The shortfall is likely contributed to by the observed lack of an intact ROS which should have served as a repository for the transgenic receptor. It should be noted, however, that the differential enrichment of receptor binding sites in the total homogenate (used for retinas) vs membrane (used for transfected cells) preparations used in our study leaves open the possibility that the levels of receptor binding sites actually present in retinal membranes may be much higher than those reported here and significantly higher than what might be obtained with conventional cell-based transfection systems. Additional experiments are needed using equivalent biochemical preparations from retina tissues and HEK293T cells to more accurately quantify and compare the amount of active binding sites and total receptor protein present.

In summary, our results provide a preliminary demonstration of the feasibility of expressing selected GPCR proteins in the retinal photoreceptor expression system and suggest that further exploration of this system is warranted. Optimization of the molecular constructs with regard to promoter and regulatory element usage (including the use of inducible systems), the genetic strains of animals used, and the temporal window of transgenic retinal development could all favorably impact the integrity of the ROS as a depot for GPCR proteins. Despite the absence of ROS layers in the transgenic animals described here, the usefulness of these lines for structural studies is not necessarily precluded. Recent advances in microcrystallization methods and brighter beam sources now available for X-ray diffraction studies should allow us to take maximal advantage of retinal receptor protein recoverable from transgenic mouse strains now in

hand. The results of purification and crystallization trials using these and new strains will ultimately determine the usefulness of this approach.

ACKNOWLEDGMENT

We thank Ms. Jianhua He and Mr. Tony Li for technical assistance, Mr. James McCabe for mouse breeding, the Transgenic and Targeting Facility at Case Western Reserve University for assistance in developing some of the transgenic lines used in this study, and Dr. William Harte and Dr. Paul Reider for critical discussions of this work.

REFERENCES

- Lefkowitz, R. J. (2004) Historical review: A brief history and personal retrospective of seven-transmembrane receptors, *Trends Pharmacol. Sci.* 25, 413–422.
- Thompson, M. D., Burnham, W. M., and Cole, D. E. (2005) The G protein-coupled receptors: pharmacogenetics and disease, *Crit. Rev. Clin. Lab. Sci.* 42, 311–392.
- Schlyer, S., and Horuk, R. (2006) I want a new drug: G-protein-coupled receptors in drug development, *Drug Discov. Today* 11, 481–493.
- Palczewski, K., Kumasaka, T., Hori, T., Behnke, C. A., Motoshima, H., Fox, B. A., Le Trong, I., Teller, D. C., Okada, T., Stenkamp, R. E., Yamamoto, M., and Miyano, M. (2000) Crystal structure of rhodopsin: A G protein-coupled receptor, *Science* 289, 739–745.
- Salom, D., Lodowski, D. T., Stenkamp, R. E., Le Trong, I., Golczak, M., Jastrzebska, B., Harris, T., Ballesteros, J. A., and Palczewski, K. (2006) Crystal structure of a photoactivated deprotonated intermediate of rhodopsin, *Proc. Natl. Acad. Sci. U.S.A.* 103, 16123–16128.
- Ridge, K. D., and Palczewski, K. (2007) Visual rhodopsin sees the light: structure and mechanism of G protein signaling, *J. Biol. Chem.* 282, 9297–9301.
- Palczewski, K. (2006) G protein-coupled receptor rhodopsin, *Annu. Rev. Biochem.* 75, 743–767.
- Okada, T., Le Trong, I., Fox, B. A., Behnke, C. A., Stenkamp, R. E., and Palczewski, K. (2000) X-Ray diffraction analysis of three-dimensional crystals of bovine rhodopsin obtained from mixed micelles, *J. Struct. Biol.* 130, 73–80.
- Deretic, D. (2006) A role for rhodopsin in a signal transduction cascade that regulates membrane trafficking and photoreceptor polarity, *Vision Res.* 46, 4427–4433.
- Filipek, S., Stenkamp, R. E., Teller, D. C., and Palczewski, K. (2003) G protein-coupled receptor rhodopsin: A prospectus, *Annu. Rev. Physiol.* 65, 851–879.
- Eroglu, C., Cronet, P., Panneels, V., Beauvils, P., and Sinning, I. (2002) Functional reconstitution of purified metabotropic glutamate receptor expressed in the fly eye, *EMBO Rep.* 3, 491–496.
- Eroglu, C., Brugger, B., Wieland, F., and Sinning, I. (2003) Glutamate-binding affinity of *Drosophila* metabotropic glutamate receptor is modulated by association with lipid rafts, *Proc. Natl. Acad. Sci. U.S.A.* 100, 10219–10224.
- Zhang, L., Salom, D., He, J., Okun, A., Ballesteros, J., Palczewski, K., and Li, N. (2005) Expression of functional G protein-coupled receptors in photoreceptors of transgenic *Xenopus laevis*, *Biochemistry* 44, 14509–14518.
- al-Ubaidi, M. R., Pittler, S. J., Champagne, M. S., Triantafyllos, J. T., McGinnis, J. F., and Baehr, W. (1990) Mouse opsin. Gene structure and molecular basis of multiple transcripts, *J. Biol. Chem.* 265, 20563–20569.
- Zack, D. J., Bennett, J., Wang, Y., Davenport, C., Klaunberg, B., Gearhart, J., and Nathans, J. (1991) Unusual topography of bovine rhodopsin promoter-lacZ fusion gene expression in transgenic mouse retinas, *Neuron* 6, 187–199.
- Lem, J., Applebury, M. L., Falk, J. D., Flannery, J. G., and Simon, M. I. (1991) Tissue-specific and developmental regulation of rod opsin chimeric genes in transgenic mice, *Neuron* 6, 201–210.
- Kashanchi, F., Thompson, J., Sadaie, M. R., Doniger, J., Duvall, J., Brady, J. N., and Rosenthal, L. J. (1994) Transcriptional activation of minimal HIV-1 promoter by ORF-1 protein expressed from the SalI-L fragment of human herpesvirus 6, *Virology* 201, 95–106.
- MacKenzie, D., Arendt, A., Hargrave, P., McDowell, J. H., and Molday, R. S. (1984) Localization of binding sites for carboxyl terminal specific anti-rhodopsin monoclonal antibodies using synthetic peptides, *Biochemistry* 23, 6544–6549.
- Brinster, R. L., Chen, H. Y., Trumbauer, M. E., Yagle, M. K., and Palmiter, R. D. (1985) Factors affecting the efficiency of introducing foreign DNA into mice by microinjecting eggs, *Proc. Natl. Acad. Sci. U.S.A.* 82, 4438–4442.
- Simonet, W. S., Hughes, T. M., Nguyen, H. Q., Trebasky, L. D., Danilenko, D. M., and Medlock, E. S. (1994) Long-term impaired neutrophil migration in mice overexpressing human interleukin-8, *J. Clin. Invest.* 94, 1310–1319.
- Jewell-Motz, E. A., Donnelly, E. T., Eason, M. G., and Liggett, S. B. (1998) Agonist-mediated downregulation of G alpha i via the alpha 2-adrenergic receptor is targeted by receptor-Gi interaction and is independent of receptor signaling and regulation, *Biochemistry* 37, 15720–15725.
- Zhang, X., Wensel, T. G., and Kraft, T. W. (2003) GTPase regulators and photoresponses in cones of the eastern chipmunk, *J. Neurosci.* 23, 1287–1297.
- Adamus, G., Zam, Z. S., Arendt, A., Palczewski, K., McDowell, J. H., and Hargrave, P. A. (1991) Anti-rhodopsin monoclonal antibodies of defined specificity: characterization and application, *Vision Res.* 31, 17–31.
- Ye, H., Holterman, A. X., Yoo, K. W., Franks, R. R., and Costa, R. H. (1999) Premature expression of the winged helix transcription factor HFH-11B in regenerating mouse liver accelerates hepatocyte entry into S phase, *Mol. Cell. Biol.* 19, 8570–8580.
- Zhu, L., Jang, G. F., Jastrzebska, B., Filipek, S., Pearce-Kelling, S. E., Aguirre, G. D., Stenkamp, R. E., Acland, G. M., and Palczewski, K. (2004) A naturally occurring mutation of the opsin gene (T4R) in dogs affects glycosylation and stability of the G protein-coupled receptor, *J. Biol. Chem.* 279, 53828–53839.
- Zhu, L., Imanishi, Y., Filipek, S., Alekseev, A., Jastrzebska, B., Sun, W., Saperstein, D. A., and Palczewski, K. (2006) Autosomal recessive retinitis pigmentosa and E150K mutation in the opsin gene, *J. Biol. Chem.* 281, 22289–22298.
- Breathnach, R., and Harris, B. A. (1983) Plasmids for the cloning and expression of full-length double-stranded cDNAs under control of the SV40 early or late gene promoter, *Nucleic Acids Res.* 11, 7119–7136.
- Crouch, R., Purvin, V., Nakanishi, K., and Ebrey, T. (1975) Isorhodopsin II: artificial photosensitive pigment formed from 9,13-dicis retinal, *Proc. Natl. Acad. Sci. U.S.A.* 72, 1538–1542.
- Jastrzebska, B., Fotiadis, D., Jang, G. F., Stenkamp, R. E., Engel, A., and Palczewski, K. (2006) Functional and structural characterization of rhodopsin oligomers, *J. Biol. Chem.* 281, 11917–11922.
- Rivkees, S. A., Lasbury, M. E., and Barbhayya, H. (1995) Identification of domains of the human A1 adenosine receptor that are important for binding receptor subtype-selective ligands using chimeric A1/A2a adenosine receptors, *J. Biol. Chem.* 270, 20485–20490.
- Cordeaux, Y., Ijzerman, A. P., and Hill, S. J. (2004) Coupling of the human A1 adenosine receptor to different heterotrimeric G proteins: evidence for agonist-specific G protein activation, *Br. J. Pharmacol.* 143, 705–714.
- Fredholm, B. B., Ap, I. J., Jacobson, K. A., Klotz, K. N., and Linden, J. (2001) International Union of Pharmacology. XXV. Nomenclature and classification of adenosine receptors, *Pharmacol. Rev.* 53, 527–552.
- Reeves, P. J., Callewaert, N., Contreras, R., and Khorana, H. G. (2002) Structure and function in rhodopsin: high-level expression of rhodopsin with restricted and homogeneous N-glycosylation by a tetracycline-inducible N-acetylglucosaminyltransferase I-negative HEK293S stable mammalian cell line, *Proc. Natl. Acad. Sci. U.S.A.* 99, 13419–13424.
- Chelikani, P., Reeves, P. J., Rajbhandary, U. L., and Khorana, H. G. (2006) The synthesis and high-level expression of a beta2-adrenergic receptor gene in a tetracycline-inducible stable mammalian cell line, *Protein Sci.* 15, 1433–1440.
- Lundstrom, K., Wagner, R., Reinhart, C., Desmyter, A., Cherouati, N., Magnin, T., Zeder-Lutz, G., Courtot, M., Prual, C., Andre, N., Hassaine, G., Michel, H., Cambillau, C., and Pattus, F. (2006) Structural genomics on membrane proteins: comparison of more

- than 100 GPCRs in 3 expression systems, *J. Struct. Funct. Genomics* 7, 77–91.
36. Kodama, T., Imai, H., Doi, T., Chisaka, O., Shichida, Y., and Fujiyoshi, Y. (2005) Expression and localization of an exogenous G protein-coupled receptor fused with the rhodopsin C-terminal sequence in the retinal rod cells of knockin mice, *Exp. Eye Res.* 80, 859–869.
37. Fliesler, S. J., Rapp, L. M., and Hollyfield, J. G. (1984) Photoreceptor-specific degeneration caused by tunicamycin, *Nature* 311, 575–577.
38. Fliesler, S. J., Rayborn, M. E., and Hollyfield, J. G. (1985) Membrane morphogenesis in retinal rod outer segments: inhibition by tunicamycin, *J. Cell Biol.* 100, 574–587.
39. Salom, D., Le Trong, I., Pohl, E., Ballesteros, J. A., Stenkamp, R. E., Palczewski, K., and Lodowski, D. T. (2006) Improvements in G protein-coupled receptor purification yield light stable rhodopsin crystals, *J. Struct. Biol.* 156, 497–504.
40. Humphries, M. M., Rancourt, D., Farrar, G. J., Kenna, P., Hazel, M., Bush, R. A., Sieving, P. A., Sheils, D. M., McNally, N., Creighton, P., Erven, A., Boros, A., Gulya, K., Capocchi, M. R., and Humphries, P. (1997) Retinopathy induced in mice by targeted disruption of the rhodopsin gene, *Nat. Genet.* 15, 216–219.
41. Liang, Y., Fotiadis, D., Maeda, T., Maeda, A., Modzelewska, A., Filipek, S., Saperstein, D. A., Engel, A., and Palczewski, K. (2004) Rhodopsin signaling and organization in heterozygote rhodopsin knockout mice, *J. Biol. Chem.* 279, 48189–48196.
42. Olsson, J. E., Gordon, J. W., Pawlyk, B. S., Roof, D., Hayes, A., Molday, R. S., Mukai, S., Cowley, G. S., Berson, E. L., and Dryja, T. P. (1992) Transgenic mice with a rhodopsin mutation (Pro23His): a mouse model of autosomal dominant retinitis pigmentosa, *Neuron* 9, 815–830.

BI700154H